Aiding phase unwrapping by increasing the number of residues in two-dimensional wrapped-phase distributions

MUNTHER A. GDEISAT,[1*] DAVID R. BURTON,[2] FRANCIS LILLEY [2], MIGUEL AREVALILLO-HERRÁEZ [3], MARWAN M. M. AMMOUS,[1]

[1]*Colleges of Applied Sciences, Sohar, PO BOX 135, Post Code 311, Oman (e-mail: gdeisat@hotmail.com)*
[2]*General Engineering Research Institute, Liverpool John Moores University, Liverpool L3 3AF, UK.*
[3]*Departament d'Informàtica. Universitat de València, 46100. Burjassot, Valencia, Spain.*
Corresponding author: gdeisat@hotmail.com

Received XX Month XXXX; revised XX Month, XXXX; accepted XX Month XXXX; posted XX Month XXXX (Doc. ID XXXXX); published XX Month XXXX

In phase unwrapping residues are points of locally inconsistent phase that occur within a wrapped phase map which are usually regarded as being problematic for phase unwrapping algorithms. Real phase maps typically contain a number of residues that are approximately proportional to the subsequent difficulty in unwrapping the phase distribution. This paper suggests the radical use of the discrete Fourier transform to actually increase the number of residues in 2D phase-wrapped images that contain discontinuities. Many of the additional residues that are artificially generated by this method are located on these discontinuities. For example, in fringe projection systems, such phase discontinuities may come from physical discontinuity between different parts of the object, or by shadows cast by the object. The suggested technique can improve the performance of path independent phase unwrapping algorithms because these extra residues simplify the process of setting the branch cuts in the wrapped image based on the distance to the nearest residue. The generated residues can also be used to construct more reliable quality maps and masks. The paper includes an initial analysis upon simulated phase maps and goes on to verify the results on a real experimental wrapped phase distribution.

OCIS codes: *(100.5088) Image processing, phase unwrapping;*

http://dx.doi

1. INTRODUCTION

Many signal recovery methods yield phase values that are constrained to their principal values. These are called the wrapped phase, and the process of recovering a continuous form is called phase unwrapping [1].

In many real world applications that measure the phase of a signal, phase unwrapping is an essential task. Some examples are MRI [2], [3], synthetic aperture radar (SAR) [4], [5], and interferometry [6]. The difficulty of the problem has resulted in a large number of attempts to reach acceptable solutions and hundreds of algorithms have been proposed and published. Most of these techniques can be classified into three categories: 1) path independent methods that set branch cuts to prevent the unwrapping path from crossing discontinuities, noisy areas and under-sampled regions [7], [8], [9]; 2) path dependent methods that use quality maps [10]; and 3) minimum norm methods [1], [11].

The presence of residues has been commonly associated with the existence of local inconsistencies in the phase map. Hence, they are used by some of the most effective 2D and 3D unwrapping methods to devise a path that avoids entering/crossing areas of poor quality wrapped phase. In the branch cut methods, the network of branch cuts is computed by using straight lines to join together pairs of positive and negative residues. In the quality guided methods, the distance to the nearest residue can also be used to yield a quality map of the original phase signal. This map is used to guide the construction of a minimum spanning tree that defines the unwrapping path [7].

Given that residues are indicators of poor quality regions of the phase signal, then it may be hypothesized that increasing the number of them might help in detecting and evading inconsistent phase areas. In branch-cut methods, this increase in the number of residues will reduce the distances between them, and thus simplify the process of setting branch cuts. In quality-based methods, residue density can be used as an estimator for the noise level of the wrapped phase map. This helps to determine noisy regions and unwrapping strategies here aim to unwrap the phase map by starting from areas that are less noisy, thus having the highest phase quality, as suggested in [12].

In this paper, we propose a method that uses the Fourier transform to artificially alter the location and/or the number of phase wraps in the original phase map. The purpose is to discover new residues that can be used to improve unwrapping results. One major advantage of the method is that it integrates seamlessly with existing phase unwrapping algorithms as a pre-processing step.

2. THE ALGORITHM

The following example explains the proposed algorithm. Consider the computer-generated spiral shape $\varphi(x, y)$, which is shown in Fig. 1(a) as a 3D surface and displayed in Fig. 1(b) as a visual intensity array [1]. This shape has the size of 257×257 pixels. Fig 1(c) shows the corresponding wrapped phase

signal $\varphi_w(x,y)$, which has been obtained using (1) [1].

$$\varphi_w(x,y) = \mathcal{W}[\varphi(x,y)] \\ = arctan2[sin(\varphi(x,y)), cos(\varphi(x,y))] \quad (1)$$

Where $arctan2[.]$ the four quadrant arctangent is function and $\mathcal{W}[.]$ is the phase wrapping operator. There are about 42 pixels per cycle in this example. We refer to a cycle as the number of pixels between two consecutive wraps (2π jumps). Hence the spatial frequency $f_o \approx 1/42$.

The resultant wrapped phase values have a range of [-π, π[. This simulated wrapped phase image is considered to pose a challenging unwrapping task, since it contains significant phase discontinuities [1], [13].

Residues correspond to local inconsistencies in the phase map, and are detected on every 2×2 closed path in the wrapped phase map. Residues may have the values of -1, 0 or +1 [1]. A zero value indicates the absence of a residue. Values of +1 and -1 indicate the presence of a residue with positive or negative polarity, respectively. Fig. 1(d) shows the location of residues in the wrapped phase map. White dots are used for residues with a positive polarity; whereas black dots represent negative polarity residues. There are a total of 48 residues in this simulated example and they are all located upon phase discontinuities within the wrapped phase map, as shown in Fig. 1(e). These residues can be used to place branch cuts that are used as barriers to prohibit the phase unwrapping path from passing through them. The ideal branch cut for the wrapped phase map has been drawn manually here indicated as a solid line and this is shown in Fig. 1(f). Branch-cut phase unwrapping algorithms aim is to generate this branch cut placement automatically.

The following equations convert the wrapped phase map into the complex array $\varphi_{wc}(x,y)$ [14].

$$\varphi_{wc}(x,y) = \exp[j\varphi_w(x,y)] \quad (2)$$

Where $j = \sqrt{-1}$. The 2D Fourier transform of $\varphi_{wc}(x,y)$ is calculated as shown in (3).

$$\Phi(u,v) = \mathbb{F}[\varphi_{wc}(x,y)] \quad (3)$$

Where $\mathbb{F}[.]$ is the 2D Fourier transform operator, and the terms u and v are the vertical and horizontal frequencies respectively. The 2D Fourier transform of the wrapped phase map shown in Fig. 1(c) is calculated using (2) and (3). The magnitude of the Fourier transform is shown in Fig. 1(g). The peak in the frequency domain is located at the frequencies $v_o = 6 \approx 257/42$ and $u_o = 0$.

The location and number of phase wraps can be changed using the Fourier transform as follows. First, the 2D Fourier transform of the wrapped phase map needs to be shifted in the frequency domain by u_o and v_o. Both values can be chosen arbitrary. Then the inversed 2D Fourier transform $\mathbb{F}^{-1}[.]$ is calculated to produce a second wrapped phase map.

$$\varphi_{wcs}(x,y) = \mathbb{F}^{-1}[\Phi(u-u_o, v-v_o)] \quad (4)$$

After this, a new wrapped phase map can be generated by using (5) and the $arctan2(a,b)$ function.

$$a = \Re[\varphi_{wcs}(x,y)] \quad (5a)$$
$$b = \mathcal{I}[\varphi_{wcs}(x,y)] \quad (5b)$$

Where $\mathcal{I}[.]$ represents the imaginary part, and $\Re[.]$ represents the real part of the complex array $\varphi_{wcs}(x,y)$. The new phase map generated contains a new set of residues in addition to some of the ones that were detected in the original wrapped phase map.

Fig. 1(h) shows the shifted Fourier transform $\Phi(u-u_o, v-v_o)$ using the frequency shift values $u_o = 20$ and $v_o = 20$. The new wrapped phase map is then calculated using (4), (5) and the $arctan2[.]$ function. The resultant wrapped phase map image is shown in Fig. 1(i). The residues for this image are calculated and are shown in Fig. 1(j). This process has almost tripled the number of residues in the wrapped phase map, as there are now 143 residues present which are also positioned along the phase discontinuities as shown in Fig. 1(k). In addition, most of these residues are actually different from the original ones that were shown in Fig. 1(d) and only 27 of these residues are located at the original positions. A combination of both residues' images, shown in Figs. 1(d) and 1(j) respectively, yields a new residues' image that contains 164 residues.

The newly artificially added residues can be used to construct quality maps or branch cuts or mask, which may then be used to help in unwrapping the original wrapped phase distribution shown in Fig. 1(c).

The wrapped phase map shown in Fig 1(c) was unwrapped using Flynn's algorithm [15] which uses pseudo variance as a quality map [1]. The resultant unwrapped phase map is shown in Figs 1(l) and 1(m). The mathematical difference between the spiral object and the unwrapped phase is shown in Figs. 1(n) and 1(o) in radians. Comparing the continuous spiral object shown in Figs. 1(a) and 1(b) with the unwrapped phase reveals that Flynn's algorithm failed to adequately process the wrapped phase.

The above simulation was subsequently repeated, but this time incorporating the residues generated using the suggested algorithm, shown in Fig. 1(j), are used as a mask that is provided to Flynn's algorithm. The unwrapped phase map is shown in Figs. 1(p) and 1(q). The mathematical difference between the spiral object and the unwrapped phase is shown in Figs. 1(r) and 1(s) in radians. Comparing the continuous object shown in Figs. 1(a) and 1(b) with the resultant unwrapped phase reveals that Flynn's algorithm has now partially succeeded in processing the wrapped phase map.

Computer simulation is used to evaluate the effect of noise on the proposed method. White noise with a variance of 0.25 is added to the continuous object shown in Fig. 1(a) and then it is wrapped using (1). The resultant wrapped phase map is shown in Fig. 2(a). The residues for this wrapped phase map are shown in Fig. 2(b) and the number of residues is increased to 56. This phase map is unwrapped using Flynn algorithm that uses derivative variance quality map [1]. The unwrapped phase map is shown in Figs. 2(c) and 2(d), and they show that Flynn algorithm has failed to unwrap this image. The mathematical difference between the spiral object and the unwrapped phase is shown in Figs. 2(e) and 2(f) in radians.

The above simulation is repeated for the noisy wrapped phase map using the proposed algorithm with the frequency shift values $u_o = 20$ and $v_o = 20$. The resultant wrapped phase map is shown in Fig. 2(g). The residues for this phase map are shown in Fig. 2(h) and the number of residues is increased to 149. Notice that all residues are located on the phase discontinuity.

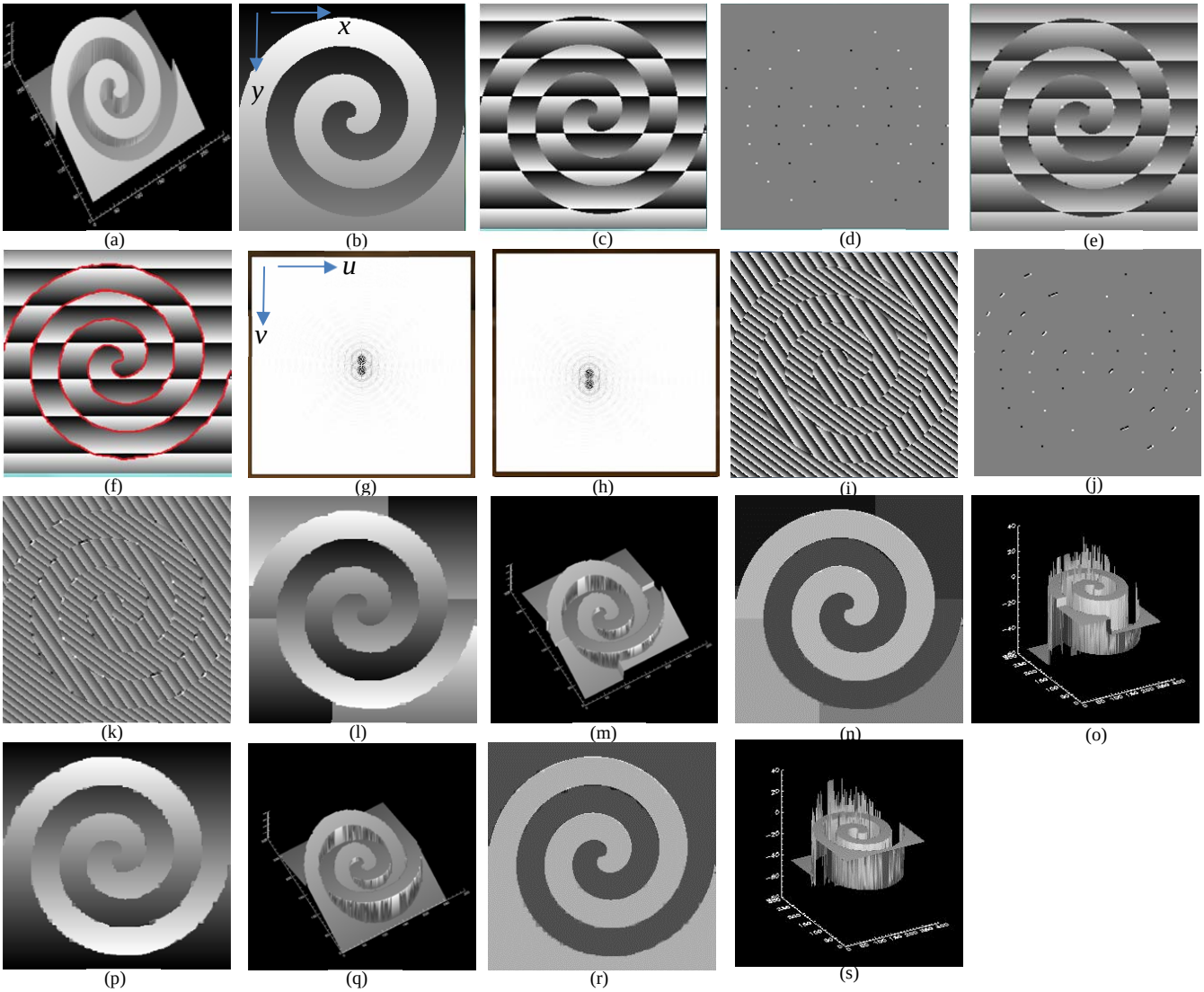

Fig. 1. The process of increasing the number of residues is shown using a simulated wrapped phase map.

The wrapped phase map shown in Fig. 2(a) is unwrapped using Flynn algorithm that uses derivative variance quality map. The residues shown in Fig. 2(h) are used as a mask by Flynn algorithm. The unwrapped phase map is shown in Figs. 2(i) and 2(j), and they show that Flynn algorithm has succeeded partially in unwrapping this image. The mathematical difference between the spiral object and the unwrapped phase is shown in Figs. 2(k) and 2(l) in radians.

In a second example, white noise with a variance of 1 is added to the continuous object shown in Fig. 1(a) and then it is wrapped using (1). The resultant wrapped phase map is shown in Fig. 2(m). This noisy wrapped phase map is processed using the proposed algorithm using (1) to (5) with $u_o = 50$, $v_o = 50$. The resultant residues are shown in Fig. 2(n). All the 385 residues are located on the discontinuity and they can be used to aid in the unwrapping process.

In a third example, noise with a variance of 3 is added to the continuous object shown in Fig. 1(a) and then it is wrapped using (1). The resultant wrapped phase map is shown in Fig. 2(o). This very noisy wrapped phase map is processed using the proposed algorithm using (1) to (5) with $u_o = 20$, $v_o = 20$. The resultant residues are shown in Fig. 2(p) and they are distributed randomly in the image. These residues cannot be used to detect phase discontinuities and should not be used to aid in the unwrapping process.

The effect of changing the horizontal frequency shift u_o and the vertical frequency shift v_o on the number of residues is shown in Fig. 2(q) as a 3D plot. Also, the effect of changing the horizontal frequency shift u_o and the variance of the added white noise σ^2 on the number of residues is shown in Fig. 2(r) as a 3D plot. Additionally, the effect of changing the vertical frequency shift v_o and the variance of the added white noise on the number of residues is shown in Fig. 2(s) as a 3D plot. These three figures show that increasing u_o, v_o and σ^2 result in increasing the number of residues.

As a rule of thumb, the proposed algorithm is useful to aid unwrapping phase maps with moderate noise levels (*i.e.,* $\sigma^2 < 1$). Also, the frequency shift should not exceed quarter the image size (*e.g.*, u_o and v_o are smaller than 64 for the image shown in Fig. 1(c)).

The noise performance of phase unwrapping algorithms may decline as the number of samples per cycle (e.g., fringe) decreases [16]. This is indicated, for the proposed algorithm, in Figs. 2(r) and 2(s) where the number of noise-induced residues increases rapidly with the increase of the frequency shifts in both u or v directions. This makes the proposed algorithm not suitable to process noisy wrapped phase maps with large spatial frequencies (e.g., $f_o > 0.1$).

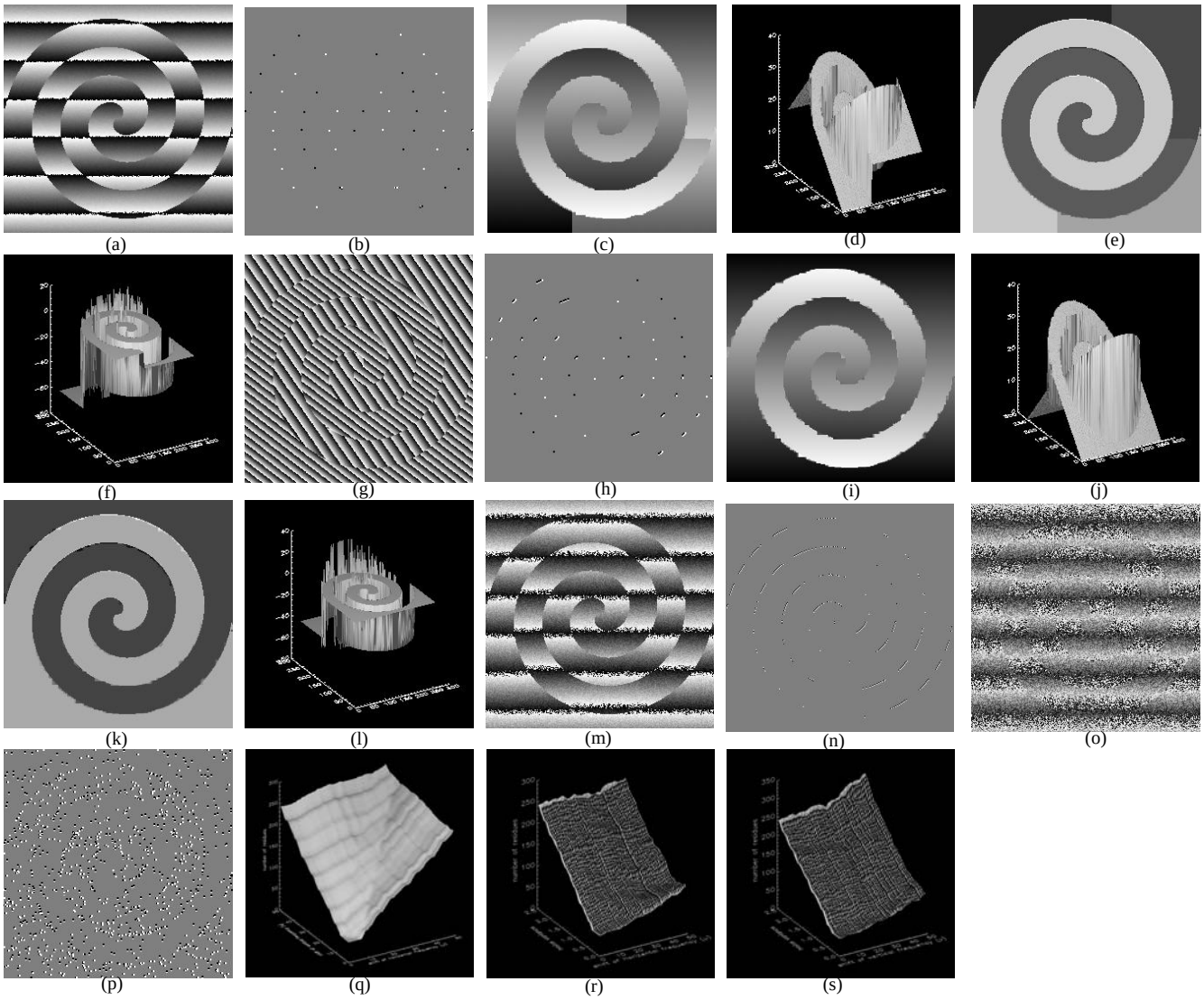

Fig. 2. Evaluating the noise performance of the proposed method.

The validity of the algorithm has also been shown experimentally. Figs. 3(a) to 3(d) show four real fringe patterns captured with a phase shift of π/2 between each of the successive images. The phase in these fringe patterns may be subsequently extracted using the well-known four-frame phase stepping algorithm, using (6) [17].

$$\varphi_w(x,y) = arctan2\left(\frac{I_1(x,y)-I_3(x,y)}{I_4(x,y)-I_2(x,y)}\right) \qquad (6)$$

Where $I_1(x,y)$ refers to the fringe pattern shown in Fig. 3(a), $I_2(x,y)$ refers to the fringe pattern shown in Fig. 3(b), and so on. The extracted wrapped phase distribution is shown in Fig. 3(e). The residues for this wrapped phase map are calculated using (3) and are shown in Fig. 3(f).

The Fourier transform $\Phi(u,v)$ for this wrapped phase map is calculated using (2) and (3); and then the frequency is shifted using the values $u_o = 30$ and $v_o = 20$. The new wrapped phase map $\varphi_{wcs}(x,y)$ is calculated using (4) and (5) and the resultant phase image is shown in Fig. 3(g). The residues for this wrapped phase map are calculated and are shown in Fig. 3(h).

It evident that the proposed algorithm has generated a set of new residues that are located along the phase discontinuities.

The wrapped phase map shown in Fig. 3(e) was unwrapped using the Goldstein algorithm [7] that uses phase derivative variance as a quality map [1]. The resultant unwrapped phase map is shown in Fig. 3(i).

The above experiment was repeated, but this time using the increased number of residues generated by the proposed algorithm, which are shown in Fig. 3(h). These residues are used as a mask that is provided to guide the Goldstein algorithm. The resulting unwrapped phase map produced by this method is shown in Fig. 3(j). Comparing both unwrapped phase maps in Figs 3(i) and 3(j) reveals that using the generated residues as a mask has considerably improved the performance of the Goldstein algorithm.

It is not guaranteed that quality guided phase unwrapping algorithms converge to a unique solution, but they have been found to be reliable in practical applications [1]. This also is applied to the suggested algorithm in this paper. Conversely, global phase unwrapping algorithms, such as minimum L^p norm methods can converge to a solution [1].

3. CONCLUSION

This paper suggests a new method to increase the number of residues in a wrapped phase map. The technique can be used as a pre-processing step and integrated into existing methods that use either the location of residues to build branch cuts and/or the residue density to estimate phase noise/quality.

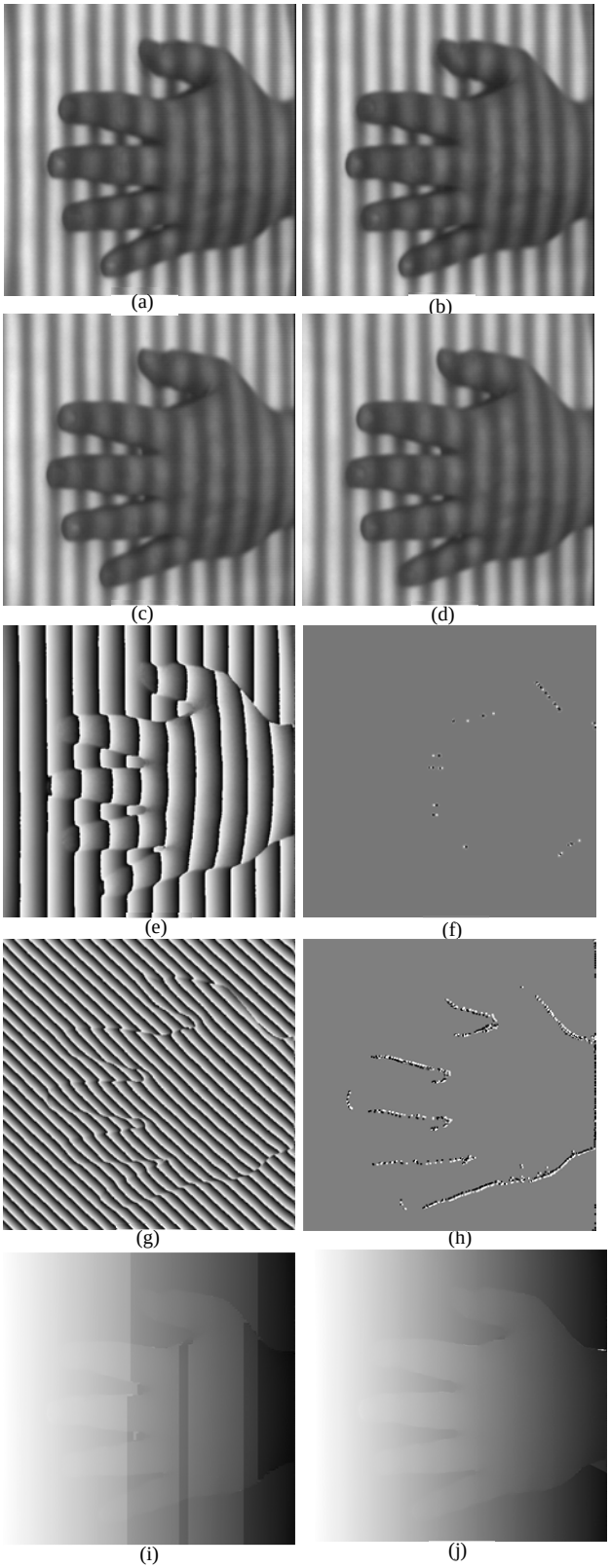

Fig. 3. The process of increasing the number of phase residues shown using a real experimental wrapped phase map.

References

1. D. Ghiglia, M. Pritt, Two-Dimensional Phase Unwrapping Theory, Algorithms and Applications (John Wiley & Sons, 1998).
2. A. Fan, S. Govindarajan, R. Kinkel, N. Madigan, A. Nielsen, T. Benner, E. Tinelli, B. Rosen, E. Adalsteinsson, C. Mainero, "Quantitative oxygen extraction fraction from 7-Tesla MRI phase: reproducibility and application in multiple sclerosis," Journal of Cerebral Blood Flow & Metabolism **35**, 131–139 (2014).
3. T. Kaaouana, T. Samaille, N. Thierry, C. Dufouil, Delmaire, D. Dormont, M. Chupin, "Phase contrast MRI for discriminating brain microbleed in a multicentre clinical study," in 1st International Conference on Advanced Technologies for Signal and Image Processing (ATSIP), 265 – 270 (2014).
4. X. Xie, P. Huang, Q. Liu, "Phase unwrapping algorithm based on extended particle filter for SAR interferometry, IEICE TRANSACTIONS on Fundamentals of Electronics, Communications and Computer Sciences **E97-A**, 405-408 (2015).
5. H. Zhong, J. Tang, S. Zhang, X. Zhang, "A quality-guided and local minimum discontinuity based phase unwrapping algorithm for InSAR/InSAS interferograms," IEEE Trans. Geoscience and Remote Sensing Letters **11**, 215 – 219 (2014).
6. K. Falaggis, D. Towers, C. Towers, "Generalized phase unwrapping for multi-wavelength interferometry," Fringe13 Conference, Germany, 653-656 (2013).
7. R. Goldstein, H. Zebker, C. Werner, "Satellite radar interferometry: two-dimensional phase unwrapping," Radio Science **23**, pp. 713-720 (1998).
8. H. Zebker, Y. Lu, "Phase unwrapping algorithms for radar interferometry: residue-cut, least-squares, and synthesis algorithms," J. Opt. Soc. Am. A.**15**, 586-598 (1988).
9. J. M. Huntley, J. R. Buckland, "Characterization of sources of 2π phase discontinuity in speckle interferograms," J. Opt. Soc. Am. A. **12**, 1990-1996 (1995).
10. G. Liu, W. R., Y. Deng, R. Chen, Y. Shao, Z. Yuan, "A new quality map for 2-D phase unwrapping based on gray level co-occurrence matrix," IEEE Trans. Geoscience and Remote Sensing Letters **11**, 444 – 448 (2014).
11. M. D. Pritt, "Phase unwrapping by means of multigrid techniques for interferometric SAR," IEEE Transactions on Geoscience and Remote Sensing **34,** 728 – 738 (1996).
12. R. Cusack, N. Papadakis, "New robust 3-D phase unwrapping algorithms: application to magnetic field mapping and undistorting echoplanar Images," NeuroImage **16**, 754–764 (2002).
13. Y. Wang, H. Huang, M. Wu, "A new phase unwrapping method for interferograms with discontinuities," IEEE Radar Conference, China, May, 56-59 (2014).
14. M. Qudeisat, M. Gdeisat, D. Burton, F. Lilley, "A simple method for phase wraps elimination or reduction in spatial fringe patterns," Optics Communications **284**, 5105–5109 (2011).
15. T. J. Flynn, "Two-dimensional phase unwrapping with minimum weighted discontinuity," Journal of the Optical Society of America A **14**, 2692-2701 (1997).
16. K. A. Stetson, J. Wahid, and P. Gauthier, "Noise-immune phase unwrapping by use of calculated wrap regions, Appl. Opt. **36**, 4830-4838 (1997).
17. K. Creath K., "Temporal phase measurement methods," in *Interferogram Analysis: Digital Fringe Pattern Measurement Techniques*, R. Robinson and G. T Reid., eds. (Institute of Physics Publishing, Bristol and Philadelphia, 1993), pp. 94-140.